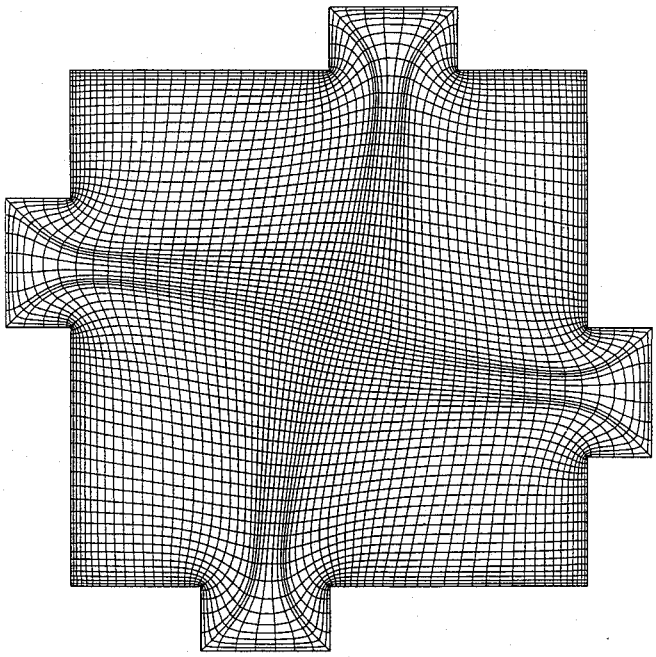

Fig. 3 Final grid system combining Fig. 8a and those starting from the right, bottom, and upper boundaries, $a = 2$ and $k = 1.4$.

The range of $1 < k < 1.5$ is employed to guarantee grid orthogonality at points next to a boundary and remote from a corner.

Results and Discussion

Figure 1 is a typical example of the application of Eqs. (3–6), which march from the lower boundary toward the upper boundary with the Hoffmann floating boundary conditions[3] on the left and right boundaries. The required CPU time is 0.2 s on a SUN Sparc X workstation and the grid size is 51 × 20. The targeting grid points along the upper boundary are vertical projections of the grid points on the $\eta = n\Delta\eta$ line. The Jacobian is then determined by specifying grid spacing along the vertical connecting line, which obviously has the effect of adjusting grid lines to fit the upper boundary. Grid smoothness around the lower and upper corners of the backward facing step is satisfactory. If only Eqs. (3) and (4) are employed, three drawbacks (not shown here) occur: the grid line will run out of the boundary in the upper corner, the grid line stemming from the upper corner will have a minor oscillation, and grid lines will cluster around the grid line stemming from the lower corner.

Figure 2 is the (x_l, y_l) grid system generated by the present grid solver whose grid size is 58 × 58. The targeting boundary is assumed to be a straight line. The grid systems generated from the bottom, right, and upper boundaries are rotational forms of Fig. 2. The result (see Fig. 3), which combines these figures and uses $a = 2$, $k = 1.4$, spent 3.0 CPU s. The grid orthogonality around all of the boundaries is preserved very well. In the central region, although grid orthogonality can not be preserved, grid points are smoothly distributed as shown.

Conclusions

A predictor-corrector version of the hyperbolic grid solver of Tai et al. is employed to construct a grid combination method for the internal flow problems. The resulting grid system preserves grid orthogonality around all of the boundaries and preserves grid smoothness in the interior region. The extension of the present study to three dimensions is simple and straightforward.

Acknowledgment

This research was supported by National Science Council of Taiwan Grant 83-0401-E006-006.

References

[1]Thompson, J. F., Thames, F. C., and Mastin, C. W., "Boundary-Fitted Coordinate Systems for Numerical Solution of Partial Differential Equations—A Review," *Journal of Computational Physics*, Vol. 47, No. 1, 1982, pp. 1–108.

[2]Steger, J. L., and Chaussee, D. S., "Generation of Body-Fitted Coordinates Using Hyperbolic Partial Differential Equations," *SIAM Journal on Scientific and Statistical Computing*, Vol. 1, No. 4, 1980, pp. 431–437.

[3]Hoffmann, K. A., Rutledge, W. H., and Rodi, P. E., "Hyperbolic Grid Generation Techniques for Blunt Body Configurations," *Numerical Grid Generation in Computational Fluid Mechanics, 88*, edited by S. Sengupta, J. Häuser, P. R. Eiseman, and J. F. Thompson, 1988, pp. 147–156.

[4]Klopfer, G. H., "Solution Adaptive Meshes with A Hyperbolic Grid Generator," *Numerical Grid Generation in Computational Fluid Mechanics, 88*, edited by S. Sengupta, J. Häuser, P. R. Eiseman, and J. F. Thompson, 1988, pp. 443–453.

[5]Chan, W. M., and Steger, J. L., "Enhancements of a Three-Dimensional Hyperbolic Grid Generation Scheme," *Applied Mathematics and Computations*, Vol. 51, No. 1, 1992, pp. 181–205.

[6]Steger, J. L., and Rizk, Y. M., "Generation of Three-Dimensional Body Fitted Coordinates Using Hyperbolic Partial Differential Equations," NASA TM 86753, June 1985.

[7]Tai, C. H., Yih, S. L., and Soong, C. Y., "A Novel Hyperbolic Grid Generation Procedure with Inherent Adaptive Dissipation," *Journal of Computational Physics* (to be published).

[8]Roe, P. L., "Approximate Riemann Solvers, Parameters, and Difference Schemes," *Journal of Computational Physics*, Vol. 43, No. 2, 1981, pp. 357–372.

[9]Jeng, Y. N., and Shu, Y. L., "On a Smoothing Technique of the Grid Distribution for the Hyperbolic Grid Solver," *Proceedings of the 2nd National Conference on Computational Fluid Dynamics*, AASRC, Taiwan, ROC, 1993, pp. 481–484.

[10]Jeng, Y. N., Shu, Y. L., and Lin, W. W., "On Grid Generation for Internal Flow Problems by Methods Solving Hyperbolic Equations," *Numerical Heat Transfer* (to be published).

[11]Jeng, Y. N., and Liou, Y. C., "Adaptive Grid Generation by Elliptic Equations with Grid Control at all of the Boundaries," *Numerical Heat Transfer*, Pt. B, Vol. 23, No. 1, 1993, pp. 135–151.

[12]Jeng, Y. N., and Liou, Y. C., "A New Adaptive Grid Generation by Elliptic Equations with Orthogonality at all of the Boundaries," *J. Sci. Comput.*, Vol. 7, No. 1, 1992, pp. 63–80.

Semi-Infinite Channel Flows Past a Cylindrical Body: A Numerical Study

J.-H. Chen*
National Taiwan Ocean University, Keelung 202, Taiwan, Republic of China

Introduction

THE two-dimensional flow past around a circular cylinder has always been an interesting problem due to its simple geometry but complicated physical phenomena. Traditionally, the study is based on flows in an infinite domain with a uniform incoming velocity far upstream. Much experimental data are available in the literature (see, for example, Ref. 1).

Although variations of the flow pattern are easily observed in experiments, few detailed reports on numerical examinations and theoretical studies are available (e.g., Refs. 2 and 3). In fact, it is difficult to simulate these flow phenomena rigorously. This arises, in part, because the decay of wake is not clearly understood and, therefore, no mathematically or physically rigorous downstream boundary conditions are known.

To avoid this difficulty, this study attempts to examine the flow by placing the cylinder in the entrance region of a semi-infinite channel flow. The emergence of the recirculating region is studied and the results are compared with those in an unbounded flow domain.

Received April. 29, 1993; presented as Paper 93-3062 at the AIAA 24th Fluid Dynamics Conference, Orlando, FL, July 6–9, 1993; revision received Sept. 10, 1994; accepted for publication Sept. 20, 1994.

*Associate Professor, Department of Naval Architecture. Member AIAA.

Problem Definition and Numerical Formulation

A uniform flow of magnitude U enters a semi-infinite channel of width w and passes a circular cylinder of diameter $d < w$ and with its center on the centerline of the channel. The origin of the coordinate is set at the center of the cylinder. The flow is governed by the incompressible Navier–Stokes equations. The dynamic parameter, the Reynolds number, is defined as $Re = U_{ave}w/\nu$. In addition, we have a geometric parameter, the blockage ratio, as $B = d/w$, which may affect the flow development.

To specify the velocity boundary conditions, we prescribe a uniform distribution at the entrance, $x = x_u$, and a fully-developed parabolic distribution at some distance $x = x_d$ downstream of the cylinder. The specification of a downstream condition at a finite distance away from the cylinder, to represent effectively the flow in an infinite domain in the streamwise direction, has been justified by the work by Amick[4] when Re is sufficiently small. In numerical simulations, this property provides a solid background for the domain truncation in the streamwise direction.

A penalty finite element method was employed throughout the study to reduce computational load. The standard second-order enriched Crouzeix–Raviart $P_2^+ - P_1$ triangular finite element scheme[5] was used to compute solutions of the discretized perturbed Navier–Stokes equations.

To solve the resulted nonlinear algebraic equation system, the method of fixed point iteration was used for the first several iterations, and then a quasi-Newton method was subsequently employed to accelerate convergence of iterations. The linearized system was then solved by lower-upper (LU) decomposition technique. The penalty parameter was set at values between 10^{-6} and 10^{-9}, depending on the size of the mesh.

Computation Procedure

It is difficult by computation to determine directly the exact Reynolds number Re_r above which the recirculation flow begins to appear. In fact, it can be quite tricky to estimate accurately the extent of the recirculating region when it is small, unless a very fine mesh is employed. Therefore, an extrapolation procedure was employed to estimate Re_r.

For each value of B, the flowfield was computed at several Reynolds numbers. Then the end point of the recirculation region on the centerline was determined by an interpolation of the computed velocity field on the centerline. After lengths at different Reynolds numbers had been calculated, a curve of the eddy length L as a function of the Reynolds number Re was fitted and extrapolated to estimate Re_r. Since, in this study, this function was found to conform very closely to a straight line, a linear relation was assumed and the least-squares criterion was employed to determine Re_r.

Computational Tests and Results

First of all, the streamwise domain truncation is an important geometrical feature possibly affecting the accuracy of the solution. To ensure that the truncated domain represents a good approximation to the semi-infinite one, a series of tests were conducted in differently truncated domains. In all computations, the cylinder was placed within the entrance region so that the core of the flow past the cylinder is approximately uniform.

Figure 1 shows the effects of upstream boundary location on the downstream flow development on the centerline for $B = 0.5$ and $Re = 40$. It is obvious that the flow at the rear of the cylinder is not noticeably disturbed. This, in turn, indicates that Re_r is not significantly affected by the location of the cylinder in the entrance region. Further numerical experiments for different blockage ratios and Reynolds numbers all agree with this finding.

For tests of the downstream boundary location, the flow with $B = 0.5$ was again studied. Flows at $Re = 80$ were computed. Figure 2 shows the u-velocity distribution along the centerline for various computational domains. Even though the flow developments near the downstream boundary differ significantly, one cannot tell one distribution from others at the immediate rear of the cylinder. These results indicate that the eddy length is not strongly influenced by the computational domain if the domain is long enough to accommodate the development of the closed recirculating flow, though the flow

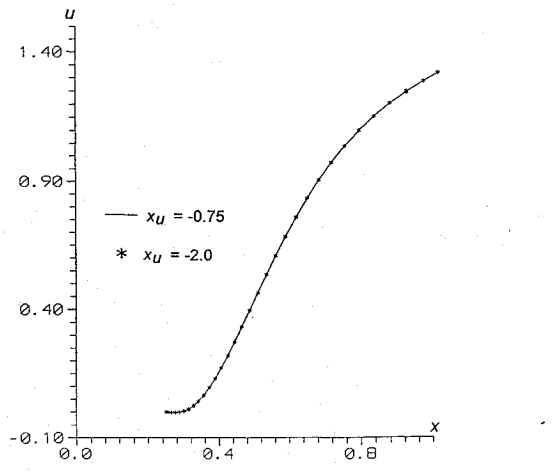

Fig. 1 Comparison of centerline velocity distribution for different locations of the upstream boundary, $Re = 40$, $x_d = 4.0$, and $B = 0.5$.

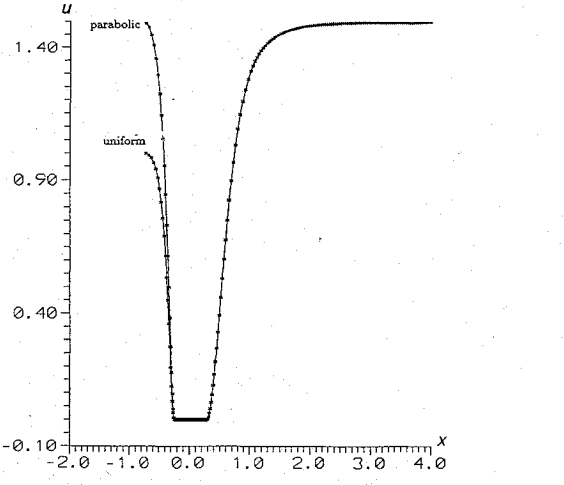

Fig. 2 Effects of the domain length on the centerline velocity distribution at the rear of the cylinder, $B = 0.5$ and $Re = 80$.

development does depend on the locations of boundary conditions. This seems to demonstrate that the downstream boundary conditions have only local effects on the flow development.

We also conducted some investigations on the effect of the upstream boundary condition on the flow development downstream of the cylinder. For this purpose, two velocity profiles commonly encountered in experiments, i.e., the uniform and the parabolic ones, were implemented in the study. As an example, the results in Fig. 3 indicate the centerline velocity distribution at $B = 0.5$, $Re = 40$, and $x_u = -0.75$. It is evident that the effect on the centerline velocity behind the cylinder is indistinguishable. Similar results were also found for flows with $x_u = -1.5$. It appears legitimate to state that the upstream boundary velocity profiles do not sensitively affect the critical Reynolds number for the formation of the recirculating flow.

Such a phenomenon may be explained as follows. The Reynolds number is small and, thus, viscous dissipation effects over the cylinder are prominent. In addition, when the flow passes the narrow passage between the wall and the cylinder, the upstream flow structure is possibly partially destroyed. Therefore, effects of different velocity profiles are not significant.

Figure 4 shows a typical computed result ($B = 0.1$). The solid line represents the data by a least-squares regression which is used to estimate the critical Reynolds number. The parameter used to measure the effect of the mesh size on solutions is defined as $H = h_{\max}/\sqrt{l \cdot w}$, where $h_{\max}$ is the length of the longest side of a triangulation and l is the length of the truncated channel domain.

It can be seen that the length of the recirculation zone varies in a nearly linear manner with the Reynolds number, at least when Re is not too large. Thus, the linear extrapolation procedure in finding Re_r seems reasonable.

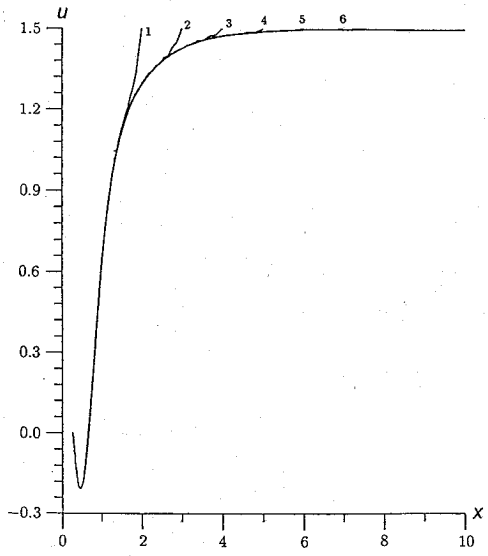

Fig. 3 Comparison of the centerline velocity distribution for different upstream velocity distributions, $Re = 40$ and $x_d = 4.0$.

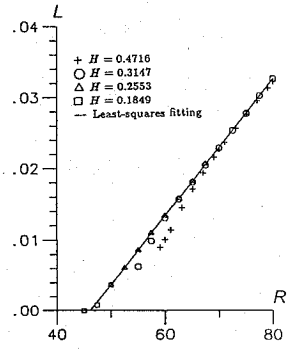

Fig. 4 Estimate of Re_r for $B = 0.1$, using meshes of different refinement; it is observed that a finer mesh is required for accurate simulation of a smaller recirculation region.

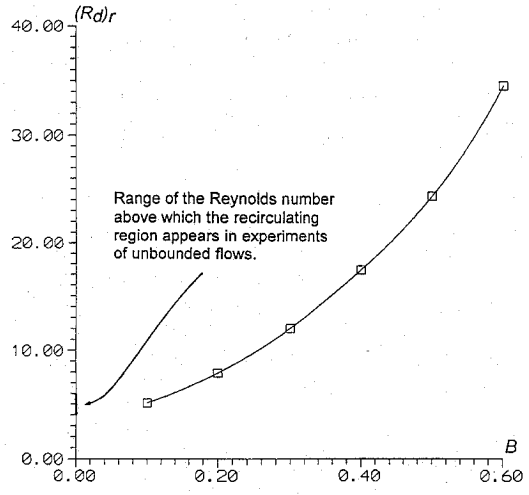

Fig. 5 $(Re_d)_r$ for different blockage ratios.

Furthermore, we define a new Reynolds number based on the diameter of the cylinder and the average speed of fluid flow at the cross section of $x = 0$,

$$Re_d := \frac{d(U_{\text{ave}})_{x=0}}{\nu} \tag{1}$$

Based on this definition, the value of $(Re_d)_r$, the Reynolds number above which the recirculation region appears, for different B is shown in Fig. 5, together with an indication of possible range of $(Re_d)_r$ in an unbounded domain. According to the trend, the curve seems to converge to the same range as B approaches zero.

Concluding Remarks

The effects of the wall boundaries on the formation of the recirculating flow of the flow past a circular cylinder have been investigated. The computed data reveal that even at a small blockage ratio, such influence is still significant. This implies that care must be exercised when truncations of a flow domain is unavoidable for computational purposes. For a careful numerical study of the flow past a circular cylinder, it seems that the value of B should not exceed 0.05, or even smaller.

In addition, it is also noticed that the uniform and parabolic velocity distribution at the upstream boundary do not lead to different centerline velocity profiles at the rear of the cylinder. Therefore, the upstream velocity distribution does not affect Re_r because at this stage the Reynolds number is small and the viscous dissipation over the cylinder is strong.

Acknowledgment

The author wishes to express his appreciation to the National Science Council of the Republic of China for the financial support of this work through Project NSC 80–0410-E-019-10.

References

[1]Taneda, S., "Experimental Investigation of the Wakes Behind Cylinders and Plates at Low Reynolds, Numbers," *Journal of the Physical Society of Japan*, Vol. 11, No. 3, 1956, pp. 302–307.

[2]Fornberg, B., "Steady Viscous Flow past a Circular Cylinder up to Reynold Number 600," *Journal of Computational Physics*, Vol. 61, No. 2, 1985, pp. 297–320.

[3]Smith, F. T., "Laminar Flow of an Incompressible Fluid past a Bluff Body: The Separation, Reattachment, Eddy Properties and Drag," *Journal of Fluid Mechanics*, Vol. 92, 1979, pp. 171–205.

[4]Amick, C. J., "Properties of Steady Navier–Stokes Solutions for Certain Unbounded Channels and Pipes," *Nonlinear Analysis, Theory, Methods, and Applications*, Vol. 2, No. 6, 1978, pp. 689–720.

[5]Crouzeix, M., and Raviart, P.-A., "Conforming and Non-Conforming Finite Element Methods for Solving the Stationary Stokes Equations," *Revue Française d'Automatique Informatique et Recherche Opérationelle*, Vol. R-3, No. 1, 1973, pp. 33–76.

Interaction of a Ribbon's Wake with a Turbulent Shear Flow

B. Chebbi* and S. Tavoularis†
University of Ottawa,
Ottawa K1N 6N5, Ontario, Canada

FOR nearly two decades, considerable attention has been given to thin ribbons or airfoils inserted in turbulent boundary layers (TBL) and their effects on the turbulence structure. Although the use of such devices for drag reduction does not appear very promising, their potential application in the reduction of noise, pressure fluctuations, and heat transfer still appears feasible. Recent investigations have attributed the observed decrease in skin friction to the reduction of the mean shear near the wall, caused by the ribbon's wake, and have demonstrated that small eddies generated in the wake attenuate the energy of the larger eddies and that the thin wake acts to isolate the inner and outer regions of the TBL. The structure of TBL is very complex. Besides producing the mean shear due to friction, the wall also imposes a kinematic constraint. Other influencing factors are turbulent transport and entrainment of the freestream fluid. Measurements in manipulated TBL are often of limited accuracy and hard to interpret, being frustrated by wall interference, severe requirements in spatial resolution, and wall curvature, as in flows

Received Feb. 25, 1994; revision received Aug. 18, 1994; accepted for publication Sept. 6, 1994.

*Research Assistant, Department of Mechanical Engineering.
†Professor, Department of Mechanical Engineering.